Landmark-based 3D Elastic Registration of Pre- and Postoperative Liver CT Data
An Experimental Comparison

Thomas Lange[1], Stefan Wörz[2], Karl Rohr[2], Peter M. Schlag[3]

[1]Experimental and Clinical Research Center, Charité–Universitätsmedizin Berlin
[2]University of Heidelberg, BIOQUANT, IPMB, and DKFZ Heidelberg,
Dept. Bioinformatics and Functional Genomics, Biomedical Computer Vision Group
[3]Charité Comprehensive Cancer Center, Charité–Unversitätsmedizin Berlin
thomas.lange@charite.de

Abstract. The qualitative and quantitative comparison of pre- and postoperative image data is an important possibility to validate computer assisted surgical procedures. Due to deformations after surgery a non-rigid registration scheme is a prerequisite for a precise comparison. Interactive landmark-based schemes are a suitable approach. Incorporation of a priori knowledge about the anatomical structures to be registered may help to reduce interaction time and improve accuracy. Concerning pre- and postoperative CT data of oncological liver resections the intrahepatic vessels are suitable anatomical structures. In addition to using landmarks at vessel branchings, we here introduce quasi landmarks at vessel segments with anisotropic localization precision. An experimental comparison of interpolating thin-plate splines (TPS) and Gaussian elastic body splines (GEBS) as well as approximating GEBS on both types of landmarks is performed.

1 Introduction

The validation of new computer-assisted surgical procedures in oncological liver surgery like preoperative planning [1] and intraoperative navigation [2] is challenging. The main question is, how accurate a resection plan has been implemented in the operating room. Besides complete tumor removal it is very important to resect exactly the planned parts of the liver vessels to ensure blood supply and drainage of the remaining liver tissue. The comparison of planned and resected tissue volumes [3] is only a coarse and unspecific validation possibility. A more detailed validation by determining the remaining vessel parts can be obtained based on pre- and postoperative CT data (Fig. 1a, b). The aim is to visualize and quantify those vessel parts, which have been resected as planned and those, which have been accidentally removed (Fig. 1c). Due to deformations of the liver between pre- and postoperative CT acquisitions non-rigid registration algorithms are needed. The challenge of this intra-patient registration task is due to the fact that significant parts of the liver are missing in the postoperative images.

Although some publications exist dealing with liver registration only few work has been published on non-rigid registration of pre- and postoperative image data. In some publications image data of the brain before and during/after resection of tumors [4, 5] are compared. In the case of the liver only the evolution of tumors of the same patient based on two different image acquisitions, but not the resection of tumors has been considered [6]. The algorithm of Charnoz et al. [6] finds corresponding vessel center lines via tree matching, but until now the method has been validated only on one clinical data set.

Our approach is based on interactively chosen corresponding point landmarks using different interpolation and approximation schemes based on splines. Besides the natural choice of landmarks at vessel branchings we introduce a special kind of landmarks adapted to vessel segments.

2   Materials and methods

2.1   Non-rigid landmark-based registration

In landmark-based non-rigid registration methods usually a smooth displacement function $u : \mathbb{R}^3 \to \mathbb{R}^3$ is searched, which maps n landmark positions p_i of a source image exactly to their corresponding positions q_i of the target image. This means, u has to fulfill the interpolation conditions $q_i = u(p_i)$, $i = 1, \ldots, n$. A function u can be defined to be smooth, if it minimizes a smoothing functional $S[u]$. The very common functional S^{tps} represents the bending energy of a thin plate leading to so called thin plate spline (TPS) interpolation functions [7]. The S^{tps} functional represents a relatively coarse deformation model, because transverse contraction does not lead to longitudinal dilation (see also [8]). In comparison, Gaussian elastic body splines (GEBS) [5] are derived from the Navier equation, which describes the deformation of homogeneous elastic materials leading to the corresponding smoothing functional $S^{\text{elas}}[u]$.

| (a) | (b) | (c) |
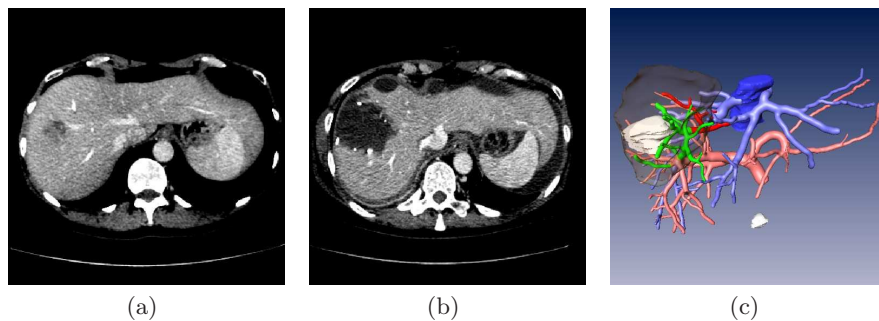
Fig. 1. a) Preoperative CT, b) Postoperative CT, c) Preoperative 3D model of liver vessels with tumor. The parts of the vessels, which have been resected as planned (green) and unnecessarily (red) have been determined by a registered postoperative 3D model. The resected tissue part is illustrated in brown.

Interpolating thin-plate splines (iTPS) and interpolating Gaussian elastic body splines (iGEBS) are analytic solutions of the following constrained optimization problem:

$$J[u] = S[u] \overset{u}{\to} \min \quad \text{subject to} \quad u(p_i) - q_i = 0, i = 1, \ldots, n \qquad (1)$$

Both *interpolation* schemes above ignore that landmark localization is generally prone to errors. Therefore, to take into account landmark errors, *approximation* schemes have been proposed (e.g., [8]). The localization uncertainties are characterized by weight matrices Σ_i representing anisotropic errors. Based on those matrices a weighted landmark distance functional can be formulated:

$$P[u] = \frac{1}{n} \int \sum_{i=1}^{n} f(x - p_i)(q_i - u(x))^T \Sigma_i^{-1} (q_i - u(x)) dx \qquad (2)$$

with a Gaussian function $f(x) = (\sqrt{2\pi}\sigma)^{-3} \exp(-\frac{\|x\|^2}{2\sigma^2})$ controlling the local influence of the landmarks on the transformation.

Instead of a constrained optimization problem like in (1), approximating GEBS (aGEBS) are formulated as an unconstrained optimization problem by adding the landmark distance functional to the smoothness functional with a weighting factor $\lambda_A \in \mathbb{R}^+$:

$$J^{\text{aGEBS}}[u] = S^{\text{elas}}[u] + \lambda_A P[u] \overset{u}{\to} \min \qquad (3)$$

2.2   Different types of landmarks for liver registration

We now describe how the presented landmark registration schemes can be applied to the registration of pre- and postoperative contrast-enhanced CTs of the liver. The main structures which are identifiable inside the liver are vessels. The vessel center lines and local radii r are usually provided by the planning process [1]. Besides landmarks at branching points of the vessel center lines, alternatively landmarks along vessels between two branchings can be used. With the latter landmarks the localization uncertainty is high along the vessel, but low perpendicular to it (Fig. 2a, b). In the following the two types of landmarks are called *branching* and *segment* landmarks. For the branching landmarks we assumed no localization uncertainty in the interpolating schemes and for the approximating scheme we assume isotropic errors $\Sigma_i = aI_3$, with $a \in \mathbb{R}$. The anisotropic error matrices of the segment landmarks can be modeled via their eigenvectors and eigenvalues. The first eigenvector $v_{i,1}$ points in the direction of the center line at the position of the landmark, the other two eigenvectors $v_{i,2}, v_{i,3}$ are perpendicular to the center line. As the localization uncertainty is high in the direction of the vessel and low perpendicular to it depending on the area of the vessel cross section, the eigenvalues are chosen as $\lambda_{i,1} = \text{const} \gg \max r_i^2, \lambda_{i,2} = r_i^2, \lambda_{i,3} = r_i^2$. With $D_i = \text{diag}(\lambda_{i,1}, \lambda_{i,2}, \lambda_{i,3})$ and $R_i = (v_{i,1}, v_{i,2}, v_{i,3})$ the uncertainty matrices are defined as $\Sigma_i = R_i^T D_i R_i$.

2.3   Design of experimental comparison

The different registration methods were compared on clinical pre- and post-operative contrast-enhanced CT data sets of 13 different patients, which have undergone oncological liver resections. For comparison we used a weighted Euclidean distance between dense point correspondences on the vessel center lines [9]. The weighting in the direction of a vessel is set to zero such that only the distance perpendicular to the vessel is measured. 5 sets of landmarks for each patient were interactively chosen as follows: 1. As many as possible branching landmark pairs (p_i^B, q_i^B), 2. a comparable number of segment landmarks on vessel segments between the branching landmarks (p_i^S, q_i^S), 3. a combination of the branching and segment landmarks (p_i^C, q_i^C), 4. a reduced number of 12 branching landmark pairs $(p_i^{B_{12}}, q_i^{B_{12}})$ and 5. a reduced number of 12 segment landmark pairs $(p_i^{S_{12}}, q_i^{S_{12}})$.

3   Results

The iTPS and iGEBS non-rigid registration approaches have been applied to landmark sets 1 and 4 which only include branching landmarks, but the aGEBS approximation was applied to all five landmark sets. The resulting average weighted Euclidean distances for each patient was determined (Fig. 2 c). On average over all patients we obtained a weighted distance of 4.9mm after rigid registration. iGEBS and aGEBS using branching landmarks decrease the average distance down to 1.7 and 1.5mm, respectively. aGEBS using segment landmarks and iTPS using branching landmarks yield comparable results and lead to 1.4mm average distance. By using a combination of segment and branching landmarks the best results of 1.0mm average distance were achieved using approximating GEBS.

Because interactive determination of landmarks is tedious and time-consuming we also performed a validation based on a reduced set of 12 landmarks.

(a)   (b)   (c)
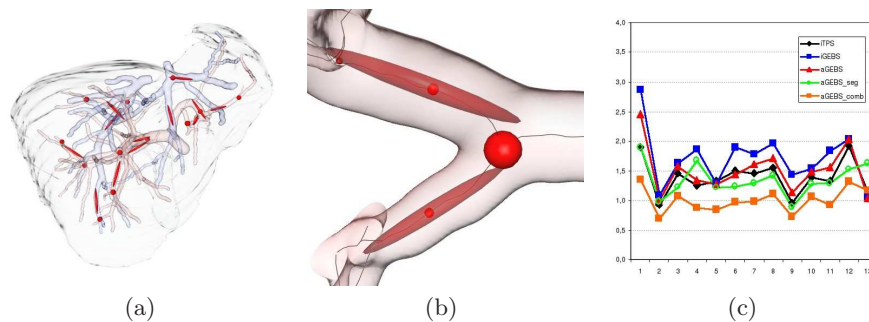
Fig. 2. a) Different types of landmarks at vessel branchings (isotropic error spheres) and segments (anisotropic error ellipsoids). b) Detailed view. c) Mean weighted Euclidean distances (in mm) after registration at vessel center lines of all 13 patients.

In this case we obtained 2.5mm for iGEBS, 2.3 mm for iTPS and aGEBS on branching landmarks and the best result of 2.0mm for aGEBS on segment landmarks.

4   Discussion

For the first time interpolating and approximating landmark-based methods have been proposed for non-rigid registration of pre- and postoperative CT data of the liver. Besides the natural choice of landmarks at vessel *branchings* also landmarks with anisotropic localization errors have been adapted to the tube-like structure of liver vessel *segments*. In an experimental comparison it turns out that the *segment* landmarks using approximating GEBS provide registration accuracies as good as *branching* landmarks and can improve the accuracy if combined with *branching* landmarks. *Segment* landmarks are even superior for a low number of landmarks. Hence segment landmarks are a promising alternative and/or extension to branching landmarks. They offer an additional flexibility in interactive landmark registration allowing an intuitive and efficient registration workflow. The registration accuracy of 2.0mm for only 12 landmarks is promising as a basis of an algorithm which automatically identifies parts of the vessel trees, which have been removed during the surgical procedure (Fig. 1c).

References

1. Selle D, Preim B, Schenk A, et al. Analysis of vasculature for liver surgical planning. IEEE Trans Med Imaging. 2002;21(11):1344–1357.
2. Beller S, Hünerbein M, Lange T, et al. Image-guided surgery of liver metastases by 3D ultrasound-based optoelectronic navigation. Brit J Surg. 2007;94(7):866–875.
3. Lemke A, Brinkmann M, Schott T, et al. Living donor right liver lobes: Preoperative CT volumetric measurement for calculation of intraoperative weight and volume. Radiology. 2006;240(3):736–742.
4. Ferrant M, Nabavi A, Macq B, et al. Serial registration of intraoperative MR images of the brain. Med Image Anal. 2002;6(4):337–359.
5. Kohlrausch J, Rohr K, Stiehl HS. A new class of elastic body splines for nonrigid registration of medical images. J Math Imaging Vis. 2005;23:253–280.
6. Charnoz A, Agnus V, Malandain G, et al. Design of robust vascular tree matching: Validation on liver. Lect Note Comp Sci. 2005;3566:443–455.
7. Bookstein FL. Principal warps: Thin-plate splines and the decomposition of deformations. IEEE Trans Pattern Anal Mach Intell. 1989;11(6):567–585.
8. Wörz S, Rohr K. Physics-based elastic registration using non-radial basis functions and including landmark localization uncertainties. Computer Vis Image Underst. 2008;111(3):263–274.
9. Lange T, Lamecker H, Hünerbein M, et al. Validation metrics for non-rigid registration of medical images containing vessel trees. Procs BVM. 2008; p. 82–86.